J Mater Sci (2011) 46:2606–2610
DOI 10.1007/s10853-010-5114-z

Crystal structure and electrical properties of $CaNaBi_2Nb_3O_{12}$ ceramics

Sunil Kumar · K. B. R. Varma

Received: 28 October 2010 / Accepted: 24 November 2010 / Published online: 8 December 2010
© Springer Science+Business Media, LLC 2010

Abstract Monophasic $CaNaBi_2Nb_3O_{12}$ powders were synthesized via the conventional solid-state reaction route. Rietveld refinement of the X-ray powder diffraction (XRD) data and selected area electron diffraction (SAED) studies confirmed the phase to be a three-layer Aurivillius oxide associated with an orthorhombic *B*2*cb* space group. The dielectric properties of the ceramics have been studied in the 300–800 K temperature range at various frequencies (1 kHz to 1 MHz). A dielectric anomaly was observed at 676 K for all the frequencies corresponding to the ferroelectric to paraelectric phase transition as it was also corroborated by the high temperature X-ray diffraction studies. The incidence of the polarization–electric field (P vs. E) hysteresis loop demonstrated $CaNaBi_2Nb_3O_{12}$ to be ferroelectric.

Introduction

Lead-based compounds are widely used for piezoelectric and ferroelectric device applications. However, toxicity of lead and related environmental concerns has compelled the researchers to look for lead-free alternatives. In lead-free materials, perovskite-type ferroelectrics such as $K_{0.5}Na_{0.5}NbO_3$, $BaTiO_3$, $Na_{0.5}Bi_{0.5}TiO_3$, etc., and bismuth-layered structure ferroelectrics (e.g., $Bi_4Ti_3O_{12}$) have been rigorously investigated in recent years [1–4]. Bismuth-layered structure ferroelectrics, also known as Aurivillius oxides, are considered to be important for non-volatile ferroelectric random access memories (Fe-RAMs) as well as for the piezoelectric device applications at high frequencies and high temperatures owing to their high ferroelectric to paraelectric transition temperatures (T_c) and good fatigue endurance [5, 6]. Structure of these oxides could be described as the regular intergrowth of $[Bi_2O_2]^{2+}$ fluorite-like layers and $[A_{n+1}B_nO_{3n+1}]^{2-}$ perovskite blocks [6]. Here A cation such as Na^+, K^+, Ca^{2+}, Sr^{2+}, Ba^{2+}, Pb^{2+}, Bi^{3+} or Ln^{3+} is in 12-fold coordination; B is in 6-fold coordination, e.g., Fe^{3+}, Ti^{4+}, Nb^{5+}, Ta^{5+} or W^{6+}; and n ($1 \le n \le 5$) represents the number of corner sharing BO_6 octahedra forming the perovskite-like slabs. Ferroelectricity in Aurivillius compounds is as a consequence of three main distortions from the prototype high temperature paraelectric phase: tilting of octahedra around the *a*- and *c*-axis and cationic displacement along the polar *a*-axis [5]. Flexibility in accommodating a variety of cations or a combination of cations at A and B sites of pseudo-perovskite block is one of the characteristic features of Aurivillius oxides. This has manifested in the synthesis of large number of Aurivillius phases with interesting properties. Number of $n = 3$ Aurivillius phases is less as compared to the other members of this family of oxides and the most studies concerning three-layer Aurivillius oxides are centred around pure and doped-$Bi_4Ti_3O_{12}$ thin films and ceramics [4, 7–10].

In a bid to search for new lead-free ferroelectrics with high Curie temperature, we have fabricated $CaNaBi_2Nb_3O_{12}$ (CNBN) ceramics using the conventional solid-state processing route. Though this phase formation was reported [11], no details pertaining to its high temperature structural, dielectric or ferroelectric properties exist in the literature. Therefore, investigations concerning the structural, dielectric, and ferroelectric properties are presented in this article.

S. Kumar · K. B. R. Varma (✉)
Materials Research Centre, Indian Institute of Science,
Bangalore 560012, India
e-mail: kbrvarma@mrc.iisc.ernet.in

Experimental

Polycrystalline calcium sodium bismuth niobate, $CaNaBi_2Nb_3O_{12}$ powder was synthesized via the conventional solid-state reaction route. For this, stoichiometric amounts of reagent grade Na_2CO_3, $CaCO_3$, Bi_2O_3, and Nb_2O_5 (purity >99%) were weighed and ball milled using agate balls in ethanol medium for 2 h. The resultant mixture was dried and calcined at 1073 K for 10 h and subsequently at 1273 K for 10 h with intermediate grinding. The calcined powders were ground again and mixed with a small amount of PVA (polyvinyl alcohol) as a binder. The mixture was uniaxially pressed into discs of about 1 mm in thickness and 10 mm in diameter. The binder was burnt out by slowly heating the pellets at 773 K for 5 h. The pressed pellets were sintered at 1323 K for 4 h in air at a heating rate of 3 K/min and then furnace cooled to room temperature.

The monophasic nature of the calcined powders and subsequently sintered pellets was confirmed by X-ray powder diffraction (Bruker-D8 Advance, Cu $K_{\alpha 1}$ radiation) studies. The FullProf program was used for Rietveld structural refinement. The Bragg peaks were modelled with pseudo-Voigt function and the background was estimated by linear interpolation between selected back-ground points. Bulk densities of the sintered ceramics were measured by the Archimedes method with xylene (density = 0.87 g/cm^3) as the liquid media. Scanning electron microscope equipped with energy dispersive X-ray spectrometry (EDXS) (Quanta-ESEM) was used for microstructural and compositional analyses. The transmission electron microscopy study was carried out with a Tecnai-T20 (200 kV) TEM equipped with a double-tilt rotating sample holder. Specimens for TEM were prepared by sonicating the dispersed polycrystalline CNBN powder in acetone medium and putting a droplet of this dispersion on a copper grid with a supported carbon thin film.

For electrical property measurements, silver electrodes were applied on either side of polished surfaces of pellet and then the sample was baked at 473 K for 2 h to dry out the moisture prior to any measurement. Capacitance and loss were measured using an impedance analyzer (Model 4194A, Hewlett-Packard) at signal strength of $0.5V_{rms}$ in the 300–800 K temperature range and at various frequencies (1 kHz to 1 MHz). All the temperature dependent experiments have been done with the measurement accuracy of ±0.5 K. The ferroelectric characteristics; the remnant polarization and coercive field were determined from the *P–E* hysteresis loop obtained using a modified Sawyer–Tower circuit (Automated PE loop tracer, Marine India Elect.).

Results and discussion

Structural and microstructural analysis

XRD powder pattern, obtained at room temperature, along with the Rietveld refinement profile for CNBN powder is shown in Fig. 1. Geguzina et al. [11], have reported (though not in detail) the $CaNaBi_2Nb_3O_{12}$ phase to crystallize in centrosymmetric space group *Fmmm*, which precludes the incidence of ferroelectricity. This is in contrast with the structure of Aurivillius oxides as these are generally known to be tetragonal (space group *I4/mmm*) in their high temperature paraelectric state while these are orthorhombic/monoclinic (class *mm2*) in their ferroelectric state as a consequence of cation displacement along the polar axis and tilting of octahedra. In the ferroelectric state, compounds associated with $n = \text{odd}$ ($Bi_4Ti_3O_{12}$)

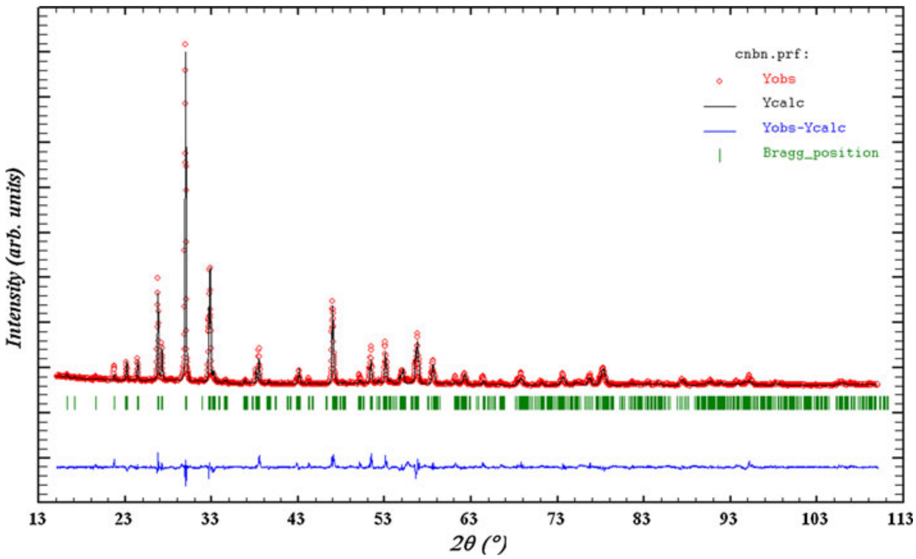

Fig. 1 X-ray diffraction pattern and the Rietveld refinement for $CaNaBi_2Nb_3O_{12}$ powders, where the *circles* are observed data points, the *solid line* is refinement result and the line below is the difference between the data points and fitted line. The *vertical bars* are the Bragg positions of the reflections in the space group *B*2*cb*

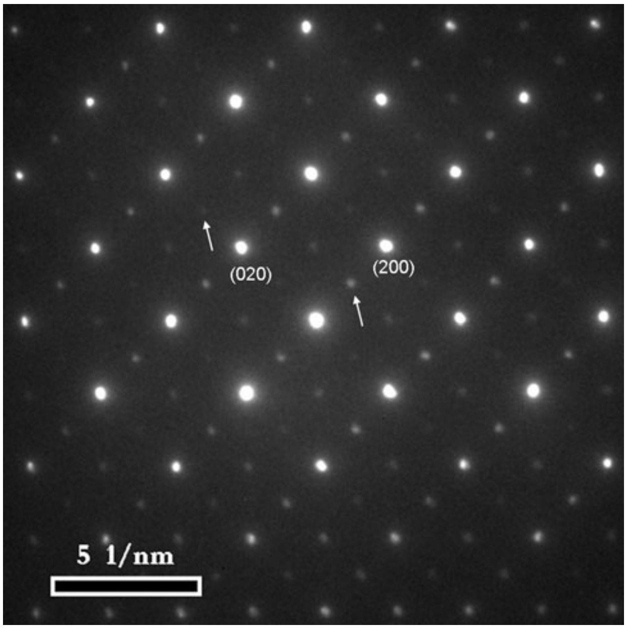

Fig. 2 SAED patterns for $CaNaBi_2Nb_3O_{12}$ along [001]

crystallize in the orthorhombic space group *B*2*cb*, whereas compounds with $n =$ even (Bi_3TiNbO_9, $BaBi_4Ti_4O_{15}$) crystallize in the orthorhombic space group $A2_1am$ [5, 6, 12, 13]. In view of the above and the fact that the present compound is indeed ferroelectric at room temperature, we carried out a detailed structural investigation. The crystal structure refinement confirms that all the diffraction peaks can be well indexed associated with the space group *B*2*cb*. The refined lattice parameters are $a = 5.4837$ Å, $b = 5.4555$ Å, and $c = 32.7437$ Å. In complement to XRD results, selected area electron diffraction (SAED) patterns were recorded. A near 4-fold SAED pattern taken along the [001] zone axis is shown in Fig. 2. Weak superlattice reflections arising due to the octahedral tilting are indicated by the arrows. It must be noted here that the *hk*0 reflections with h = odd are forbidden due to the crystallographic symmetry of *B*2*cb* space group. However, the superposition of two [001] patterns that are rotated with respect to each other by 90° around their common zone axis can give rise the diffraction spots which are evident at these positions. Diffraction spots at $2m + 1, 2n + 1, 0$, where m and n are integers, appear due to the double diffraction of electron beam. The observed SAED pattern is consistent with the one observed for $Bi_4Ti_3O_{12}$ [14].

The microstructure and the chemical composition of the sintered sample were examined by scanning electron microscope (SEM) equipped with an energy dispersive X-ray analyzer (EDX). The scanning electron micrograph recorded for the pellet sintered at 1323 K for 4 h in air is shown in Fig. 3. The micrograph shows the presence of well-packed and randomly oriented grains of various sizes ranging from 1 to 10 µm. EDX carried out on various grains of the sample confirmed the composition to be $CaNaBi_2Nb_3O_{12}$ within the typical error associated with EDX analysis. The relative density of this pellet was around 96% of theoretical density.

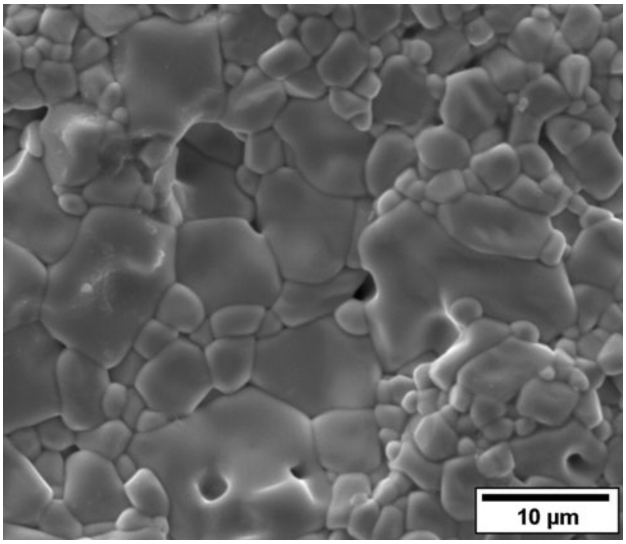

Fig. 3 Scanning electron micrograph of $CaNaBi_2Nb_3O_{12}$ ceramic sintered at 1323 K for 4 h

Dielectric properties

The temperature dependence of the dielectric constant (ε_r) and dielectric loss (D) for the pellet sintered at 1323 K for 4 h at various frequencies is depicted in Fig. 4a and b. The values of room temperature dielectric constant and loss at 1000 kHz are 120 and 0.005, respectively. CNBN (Fig. 4a) shows a diffuse maximum in the dielectric constant at 676 K at all the frequencies under investigation. This is attributed to the ferroelectric to paraelectric phase transition. The temperature of maximum is frequency independent, which confirms that CNBN is a diffuse type ferroelectric but not relaxor. Dielectric loss (Fig. 4b) also shows an anomaly at a temperature slightly lower than the transition temperature that is encountered in the dielectric constant-temperature plot. At the temperatures below 610 K, dielectric loss is lower than 0.01 (at 1000 kHz), which is useful for high temperature applications. At higher temperatures, dielectric loss of the CNBN ceramic increases significantly which lead to the strong frequency dispersion observed in dielectric constant near phase transition temperature (Fig. 4). Similar frequency dispersion in high temperature dielectric constant has been observed in other compounds belonging to the Aurivillius family of oxide [15, 16].

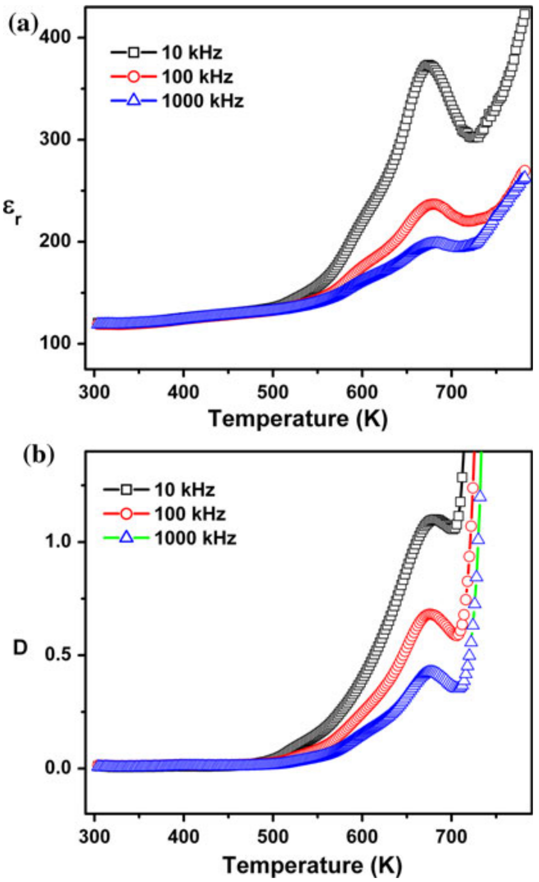

Fig. 4 Temperature dependence of **a** dielectric constant (ε_r) and **b** loss (*D*) at different frequencies

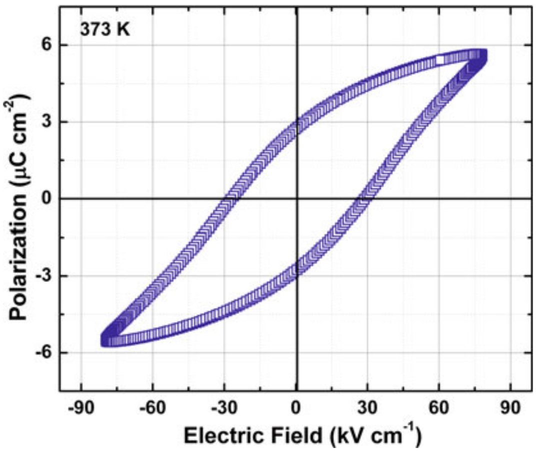

Fig. 5 Polarization–electric field (*P*–*E*) hysteresis loop for $CaNaBi_2Nb_3O_{12}$ ceramics recorded at 373 K

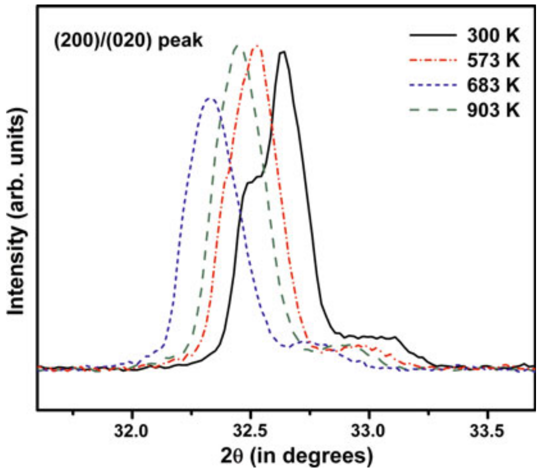

Fig. 6 Evolution of (200)/(020) XRD peaks at four different temperatures

Ferroelectric properties

To confirm the ferroelectric nature of the present compound polarization versus electric field measurements were performed at 373 K. Figure 5 shows the ferroelectric hysteresis loop obtained for CNBN ceramics. Hysteresis loop was recorded at a frequency of 50 Hz. A remnant polarization ($2P_r$) of 6 μC/cm^2 and a coercive field ($2E_c$) of 60 kV/cm were obtained under a maximum applied electric field of 79 kV/cm. However, it should be noted that the values of P_r and E_c are taken from an unsaturated loop and might be considerably higher if saturation could be reached.

High temperature X-ray studies

To investigate into the structural change occurring around the temperature of dielectric anomaly, high temperature XRD studies (room temperature to 950 K) have been carried out. The XRD peaks corresponding to (200)/(020) planes of CNBN at four different temperatures are shown in Fig. 6. The transition from orthorhombic symmetry to the tetragonal symmetry is clearly evident in the coalescence of (200)/(020) peaks. As illustrated in Fig. 6, the diffraction pattern recorded at 300 K shows splitting of the (200)/(020) reflections that is indicative of orthorhombic symmetry. With increase in temperature, peaks shift to lower angles as the lattice parameters increase. Also the splitting of the (200)/(020) peaks becomes lesser with increase in temperature. Above 670 K no splitting or diagnostic asymmetry of (200)/(020) peaks is seen. Thus, it is concluded that the dielectric anomaly around 676 K corresponds to the ferroelectric to paraelectric phase transition which is accompanied by the change in crystal structure from orthorhombic to tetragonal.

Conclusions

Single-phase $CaNaBi_2Nb_3O_{12}$ ferroelectric compound has been synthesized via solid-state reaction route. The

$CaNaBi_2Nb_3O_{12}$ crystallizes in the orthorhombic space group *B*2*cb* with $a = 5.4837$ Å, $b = 5.4555$ Å, and $c = 32.7437$ Å at room temperature. Temperature dependent dielectric properties of $CaNaBi_2Nb_3O_{12}$ ceramic have been investigated at different frequencies, which reveal a non-relaxor diffuse phase transition around 676 K. The CNBN ceramics exhibit ferroelectric hysteresis loops with a remnant polarization ($2P_r$) of 6 μC/cm^2 and a coercive field ($2E_c$) of 60 kV/cm at 373 K.

Acknowledgement One of the authors (SK) is grateful to the Council of Scientific and Industrial Research (CSIR), New Delhi, for the award of Senior Research Fellowship.

References

1. Saito Y, Takao H, Tani T, Nonoyama T, Takatori K, Homma T, Nagaya T, Nakamura M (2004) Nature 432:84
2. Rodel J, Jo W, Seifert KTP, Anton E-M, Granzow T (2009) J Am Ceram Soc 92:1153
3. Araujo CAP, Cuchiaro JD, McMillan LD, Scott MC, Scott JF (1995) Nature 374:627
4. Takenaka T, Nagata H, Hiruma Y (2008) Jpn J Appl Phys 47:3787
5. Subarao EC (1962) J Am Ceram Soc 45:166
6. Aurivillius B (1949) Ark Kemi 1:499
7. Lee HN, Hesse D, Zakharov N, Gosele U (2002) Science 296:2006
8. Cummins SE, Cross LE (1968) J Appl Phys 39:2268
9. Shrout TR, Eitel RE, Randall CA (2002) In: Setter N (ed) Piezoelectric materials in device. Ceramics Laboratory EPFL, Lausanne
10. Horn JA, Zhang SC, Selvaraj U, Messing GK, McKinstry ST (1999) J Am Ceram Soc 82:921
11. Geguzina GA, Shuvayev AT, Vlasenko VG, Shuvayeva VT, Shilkina LA (2003) Crystallogr Rep 48:406
12. Withers RL, Thompson JG, Rae AD (1991) J Solid State Chem 94:404
13. Kennedy BJ, Kubota Y, Hunter BA, Ismunandar, Kato K (2003) Solid State Commun 126:653
14. Pan XQ, Jiang JC, Theis CD, Schlom DG (2003) Appl Phys Lett 83:2315
15. Huanga S, Feng C, Gua M, Li Y (2009) J Alloys Compd 472:262
16. Sun L, Feng C, Chen L, Huang S (2007) J Am Ceram Soc 90:3875